Inorg. Chem. **2006**, *45*, 4963–4973

Computational Studies of Nucleophilic Attack and Protonation of Electron-Deficient Benzoheterocycle Triosmium Clusters

Taraneh Nowroozi-Isfahani, Djamaladdin G. Musaev,* and Keiji Morokuma*

Cherry L. Emerson Center for Scientific Computation and Department of Chemistry, Emory University, 1515 Dickey Drive, Atlanta, Georgia 30322

Edward Rosenberg*

Department of Chemistry, University of Montana, Missoula, Montana 59813

Received November 21, 2005

The density functional theory method has been applied to gain insights into the regioselectivity of nucleophilic attack and protonation of electron-deficient benzoheterocycle triosmium clusters. We report our computational results on the reaction of the green 46-electron triosmium clusters $Os_3(CO)_9(\mu_3\text{-}\eta^2\text{-}(LH))(\mu\text{-}H)$ (L = benzoxazole, **1a**; benzothiazole, **1b**; dihydroquinoline, **1c**; 1,3-dehydroindoline, **1d**; 4*H*-3,1-benzoxazine, **1e**) with hydride (H^-) and proton (H^+) in order to elucidate factors affecting the observed differences in the structure of the kinetic products of these reactions. Transition-state calculations for the interconversion of the anionic tautomers resulting from H^- attack on the clusters **1a**–**e** show that the activation energies of these anionic clusters are considerably lower than the previously reported barriers for related neutral clusters. Calculations also reveal that the structures of the kinetic products resulting from sequential H^-/H^+ attack are determined by the protonation process.

1. Introduction

Polynuclear transition-metal clusters often activate organic molecules more efficiently than mononuclear complexes, and understanding how such activation takes place is especially crucial for the development of better cluster catalysts for organic synthesis.[1] Recently, a new way of activating benzoheterocycles toward nucleophilic attack by complexation to triosmium clusters[2−5] has been introduced, which is closely related to the electron deficiency in the benzoheterocycle triosmium clusters, arising from the presence of a three-center two-electron bond in such systems.[6] The electron deficiency in these systems results in regio- and stereoselective nucleophilic attack on the carbocyclic rings where the heterocyclic rings are the site of nucleophilic attack for the free ligands. Further studies revealed that the bonding mode[6−8] of the heterocyclic ligand to the triosmium core and the nature of the heterocycles[2,5] are two important factors in determining the thermal behavior of these systems and their reactivity toward nucleophiles.

One of the interesting processes in these triosmium systems is the sequential hydride (H^-) and proton (H^+) addition to the 46-electron triosmium clusters $Os_3(CO)_9(\mu_3\text{-}\eta^2\text{-}(LH))(\mu\text{-}H)$ (L = benzoxazole, **1a**; benzothiazole, **1b**; dihydroquinoline, **1c**; 1,3-dehydroindoline, **1d**; 4*H*-3,1-benzoxazine, **1e**) containing one or two heteroatoms in (5,6) or (6,6) hetero-

* To whom correspondence should be addressed. E-mail: dmusaev@emory.edu (D.G.M.), morokuma@emory.edu (K.M.), ed.rosenberg@umontana.edu (E.R.).

(1) Shriver, D. F.; Kaesz, H. D.; Adams, R. D. *The Chemistry of Metal Cluster Complexes*; VCH Publishers, Inc.: New York, 1990.
(2) Bergman, B.; Holmquist, R. H.; Smith, R.; Rosenberg, E.; Hardcastle, K. I.; Visi, M.; Ciurash, J. *J. Am. Chem. Soc.* **1998**, *120*, 12818.
(3) Arcia, E.; Kolwaite, D. S.; Rosenberg, E.; Hardcastle, K. I.; Ciurash, J.; Duque, R.; Gobetto, R.; Milone, L.; Osella, D.; Botta, M.; Dastrú, W.; Viale, A.; Fiedler, J. *Organometallics* **1998**, *17*, 415.
(4) Kabir, S. E.; Kolwaite, D. S.; Rosenberg, E.; Scott, L. G.; McPhillips, T.; Duque, R.; Day, M.; Hardcastle, K. I. *Organometallics* **1996**, *15*, 1979.
(5) Rosenberg, E.; Abedin, J.; Kabir, S. E.; Hardcastle, K. I. *Organometallics* **2004**, *23*, 3982.
(6) Nervi, C.; Gobetto, G.; Milone, L.; Viale, A.; Rosenberg, E.; Rokhsana, D.; Fiedler, J. *Chem.—Eur. J.* **2003**, *9*, 5749.
(7) Rosenberg, E.; Rokshsana, D.; Nervi, C.; Gobetto, R.; Milone, L.; Viale, A.; Fiedler, J.; Botavina, M. A. *Organometallics* **2004**, *23*, 215.
(8) Abedin, J.; Bergman, B.; Holmquist, R.; Smith, R.; Rosenberg, E.; Ciurash, J.; Hardcastle, K. I.; Roe, J.; Vazquez, V.; Roe, C.; Kabir, S. E.; Roy, B.; Alam, S.; Azam, K. A. *Coord. Chem. Rev.* **1999**, *190−192*, 975.

10.1021/ic052012x CCC: $33.50
Published on Web 06/02/2006

Scheme 1. Nucleophilic Attack and Protonation of Triosmium Clusters $Os_3(CO)_9(\mu^3\text{-}\eta^2\text{-(LH)})(\mu\text{-H})$[a]

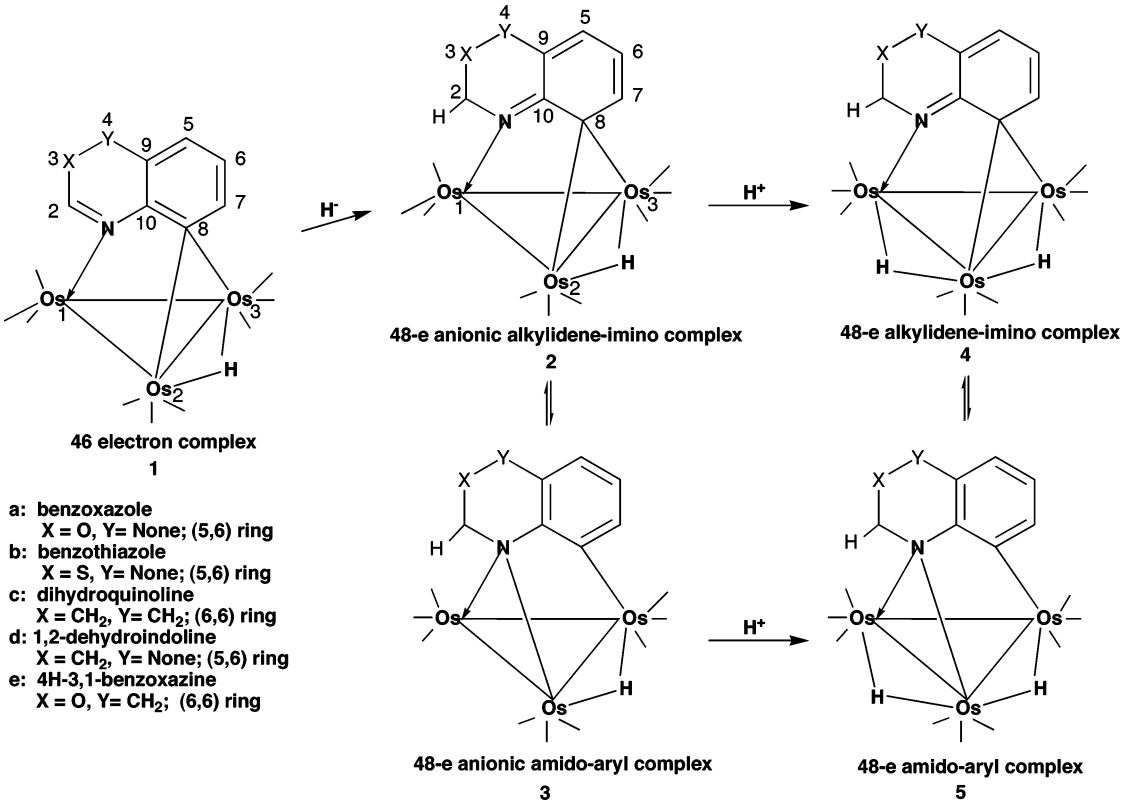

[a] The observed kinetic product for **1a** and **1b** is amidoaryl cluster **5**, and that for **1c** and **1d** is alkylideneimino cluster **4**. Experimental equilibrium constants are $k_{5a}/k_{4a} = 1.6$, $k_{5b}/k_{4b} = 3.1$, and $k_{4c}/k_{5c} = 6$. See the text for details (only the bridging H and those involved in the reaction are shown in the scheme).

cyclic rings, as shown in Scheme 1. Complexes **1d** and **1e** are hypothetical compounds constructed for the purposes of this study.

It has been observed experimentally that complexes **1a**−**c** undergo nucleophilic attack by H^- at the C2 position (see Scheme 1 for atom-numbering system) of the heterocyclic ring,[3,9] and the following protonation leads to two tautomeric 48-electron structures of μ_3-η^2-alkylideneimino $Os_3(CO)_9(\mu_3\text{-}\eta^2\text{-(L-2H)})(\mu\text{-H})_2$ (**4**) and μ_3-η^2-amidoaryl $Os_3(CO)_9(\mu_3\text{-}\eta^2\text{-(L-2H)})(\mu\text{-H})_2$ (**5**). An interesting feature of this process is the observed dependency of the structure of the kinetic products on the nature of the organic ligand. For instance, in the reaction of **1a** or **1b** with $LiEt_3BH$, the H^- attacks the C2 position, and the following protonation leads to the μ_3-η^2-amidoaryl tautomer as the kinetic product.[7] When the reaction is followed by NMR, competitive kinetic protonation is observed at the N atom and at the metal core. At 90 °C, μ_3-η^2-amidoaryl converts slowly to the thermodynamically more stable μ_3-η^2-alkylideneimino complex with equilibrium constants of 3.1 and 1.6 for **1a** and **1b**, respectively. However, the situation is reversed when treating **1c** (L = dihydroquinoline) with H^- and H^+. In this case, the μ_3-η^2-alkylideneimino complex is produced kinetically and slowly converts to the thermodynamically more stable μ_3-η^2-amidoaryl complex at 90 °C with $K_{eq} = 6$.[8]

The mechanism of H^- and H^+ addition to triosmium clusters and factors controlling the formation of a particular kinetic product during these processes, as well as details of the isomerization of the kinetic products, still remain unresolved. Although experiments have shed light on many aspects of these issues, one cannot resolve all of these problems at the atomic level by experiments alone. Computational approaches [especially hybrid density functional theory (DFT) methods such as B3LYP] have proven to be very useful in resolving such issues.[10−20] Recently, we have performed a series of relevant B3LYP studies on benzoheterocycle triosmium clusters.[9,21] This paper is a continuation of our previous studies on triosmium clusters and focuses

(9) Musaev, D. G.; Nowroozi-Isfahani, T.; Morokuma, K.; Rosenberg, E.; Abedin, J.; Hardcastle, K. I. *Organometallics* **2005**, *24*, 5973.

(10) Kim, K. H.; Jung, J.; Han, Y. K. *Organometallics* **2004**, *23*, 3865.
(11) Bergamo, M.; Beringhelli, T.; D'Alfonso, G.; Garavaglia, L.; Mercandelli, P.; Moret, M.; Sironi, A. *J. Cluster Sci.* **2001**, *12*, 223.
(12) Khoroshun, D. V.; Inagaki, A.; Suzuki, H.; Vyboishchikov, S. F.; Musaev, D. G.; Morokuma, K. *J. Am. Chem. Soc.* **2003**, *125*, 9910.
(13) Riehl, J. F.; Koga, K.; Morokuma, K. *J. Am. Chem. Soc.* **1994**, *116*, 5414.
(14) Riehl, J. F.; Koga, K.; Morokuma, K. *Organometallics* **1994**, *13*, 4765.
(15) Riehl, J. F.; Koga, K.; Morokuma, K. *Organometallics* **1993**, *12*, 4788.
(16) Zimmerman, C.; Anson, C. E.; Eckerman, A. L.; Wunder, M.; Fischer, G.; Keihauer, I.; Herrling, E.; Pilawa, B.; Hampe, O.; Weigand, F.; Dehnen, S. *Inorg. Chem.* **2004**, *43*, 4595.
(17) Wadepohl, H.; Castano, M. E. *Chem.—Eur. J.* **2003**, *9*, 5266.
(18) Morioka, T.; Ozawa, S.; Yamabe, T.; Masuda, H. *Polyhedron* **2003**, *22*, 3413.
(19) Wong, W. Y.; Choi, K. H.; Lin, Z. *Eur. J. Inorg. Chem.* **2002**, 2112.
(20) Kaupp, M. *Chem. Commun.* **1996**, 1141.
(21) Musaev, D. G.; Nowroozi-Isfahani, T.; Morokuma, K.; Rosenberg, E. *Organometallics* **2006**, *25*, 203.

on elucidation of the mechanisms of H^- and H^+ addition to the electron-deficient triosmium clusters.

2. Computational Procedure

All calculations were performed using the hybrid DFT method B3LYP[22] in conjunction with the Lanl2dz effective core potential and associated basis set[23] of Hay and Wadt for the Os atoms and 6-31(d) basis sets for the main-group elements. Below we will call this basis set Lanl2dz+6-31(d). It was previously shown that the B3LYP/Lanl2dz+6-31(d) approximation used in this paper provides reasonable agreement with available experiments and higher level methods in analogous systems.[24] However, to rationalize the adopted basis set on the geometry and energy of the species involved in the reaction, we have performed some calculations at the B3LYP level in conjunction with the Stuttgart/Dresden ECP[25] and associated triple-ζ SDD basis set for Os and the 6-31G(d) basis set for main-group elements. The results presented in the Supporting Information clearly indicate that the improvement of the basis set from Lanl2dz to SDD+6-31G(d) has no significant effect on the calculated geometries and energetics of the structures. The SDD calculation actually provides a larger error ($\sim$0.09 Å) from experimental bond lengths around the Os atoms. The energy difference between isomers **4c** and **5c** is increased by 0.1 (0.1) kcal/mol and that between anionic isomers **3c** and **3c′** is decreased by 0.2 (0.3) kcal/mol. The natural population analysis (NPA) shows an increase of the electron density at metal cores at most by 0.08e. We have also checked the influence of an additional f polarization function on Os.[26] The calculated energy difference between **3c** and **3c′** is decreased by 0.04 kcal/mol. The change in the bond length around the metal is decreased only by ca. 0.01 Å.

The harmonic vibrational frequencies of each optimized structure were calculated to identify the nature of the stationary points. Thermal corrections were calculated based on harmonic frequencies and were included in the reported energies, unless explicitly stated. Throughout the paper, the ΔH values (at 298.15 K and 1 atm) are used for comparisons of the thermodynamics of the reaction and the calculated barriers while the corresponding Gibbs free energy ΔG values will be given in parentheses. For the discussion on the rate constant calculation, ΔG is used where entropy effects are required. The standard NPA is performed to calculate the atomic charges. All calculations were performed without symmetry constraints utilizing the *Gaussian03* program.[27]

In this study, the 46-electron reactant clusters (**1a**−**e**) and the 48-electron product clusters of μ_3-η^2-alkylideneimino (**4a**−**e**) and μ_3-η^2-amidoaryl (**5a**−**e**) are neutral, while the intermediate structures of **2a**−**e**, **3a**−**e**, **3′a**, and **3′b** are hydrated anionic complexes bearing 48 electrons. In all cases, the formal oxidation states of Os atoms are considered as 0 (d^8) for electron-counting purposes.

3. Results and Discussion

Structures and Energies of the Reactants (1a and 1b) and the Overall Products (4a−e, 5a−e). As shown in Scheme 1, the organic ligands involved in the reactants studied in this paper differ mainly in two respects, the ring size and the number of heteroatoms. The dihydroquinoline cluster contains a (6,6) ring bearing pyridinyl type N, while the benzoxazole and benzothiazole clusters contain a (5,6) ring bearing pyridine type N and an additional heteroatom (O or S). Because we wanted to elucidate the effect of both the ring size and the heteroatom on the formation of **4a**−**e** and **5a**−**e** via the stepwise H^- and H^+ additions, we also studied two hypothetical clusters: **1d**, which contains a 1,3-dehydroindoline ligand and a (5,6) ring ligand with no additional heteroatom, and **1e**, 4*H*-3,1-benzoxazine, which has a (6,6) ring ligand with an additional heteroatom, O. Following attack by H^-, anionic intermediates **2a**−**e**, **3a**−**e**, and **3′a**−**e** (to be shown later) may be formed; their structures and energetics will also be studied in detail. Let us first discuss the reactants **1a**−**e** and the final products **4a**−**e** and **5a**−**e** of the sequential H^-/H^+ addition.

As seen in Figure 1, where we have presented the calculated and available experimental (in parentheses) structures of the 46-electron reactants **1a**−**e**, the calculated geometries are in good agreement with their experimental values. The calculated values of the Os−L (L is any ligand) bond lengths are about 0.04−0.07 Å longer than their experimental values. The differences between the calculated and experimental geometries of the 46-electron reactants **1a**−**e** are similar to those for **4a**−**e** and **5a**−**e** complexes discussed previously.[9]

The atomic charges from the NPA of the key atoms of complexes **1a**−**e** are summarized in Table 1. The reported charges on the C atoms are the sum of the C and H charges at each ring position. In all cases, except benzothiazole, the highest positive charge is accumulated at C2, which is consistent with the previously detailed experimental and theoretical investigations.[9] We think the lower electronegativity of S compared to O could be the reason for this exceptional behavior. Therefore, the S lone pair is in better resonance with the adjacent double bond.

Geometries of the product species **4a**−**e** and **5a**−**e** are also shown in Figure 1. These species have been discussed in detail in our previous experimental and theoretical studies.[9]

(22) (a) Becke, A. D. *J. Chem. Phys.* **1993**, *98*, 5648. (b) Lee, C.; Yang, W.; Parr, R. G. *Phys. Rev. B* **1998**, *37*, 785.

(23) (a) Dunning, T. H.; Hay, P. J. In *Modern Theoretical Chemistry*; Schaefer, H. F., III, Ed.; Plenum: New York, 1976; pp 1−28. (b) Hay, P. J.; Wadt, W. R. *J. Chem. Phys.* **1985**, *82*, 270. (c) Wadt, W. R.; Hay, P. J. *J. Chem. Phys.* **1985**, *82*, 284. (d) Hay, P. J.; Wadt, W. R. *J. Chem.Phys.* **1985**, *82*, 299.

(24) (a) Cui, Q.; Musaev, D. G.; Svensson, M.; Sieber, S.; Morokuma, K. *J. Am. Chem. Soc.* **1995**, *117*, 12366. (b) Musaev, D. G.; Morokuma, K. *J. Phys. Chem.* **1996**, *100*, 6509. (c) Erikson, L. A.; Pettersson, L. G. M.; Siegbahn, P. E. M.; Wahlgren, U. *J. Chem. Phys.* **1995**, *102*, 872. (d) Ricca, A.; Bauschlicher, C. W., Jr. *J. Phys. Chem.* **1994**, *98*, 12899. (e) Heinemann, C.; Hertwig, R. H.; Wesendrup, R.; Koch, W.; Schwarz, H. *J. Am. Chem. Soc.* **1995**, *117*, 495. (f) Hertwig, R. H.; Hrusak, J.; Schroder, D.; Koch, W.; Schwarz, H. *Chem. Phys. Lett.* **1995**, *236*, 194. (g) Schroder, D.; Hrusak, J.; Hertwig, R. H.; Koch, W.; Schwerdtfeger, P.; Schwarz, H. *Organometallics* **1995**, *14*, 312. (h) Fiedler, A.; Schroder, D.; Shaik, S.; Schwarz, H. *J. Am. Chem. Soc.* **1994**, *116*, 10734. (i) Fan, L.; Ziegler, T. *J. Chem. Phys.* **1991**, *95*, 7401. (j) Berces, A.; Ziegler, T.; Fan, L. *J. Phys. Chem.* **1994**, *98*, 1584. (k) Lyne, P. D.; Mingos, D. M. P.; Ziegler, T.; Downs, A. *J. Inorg. Chem.* **1993**, *32*, 4785. (l) Li, J.; Schreckenbach, G.; Ziegler, T. *J. Am. Chem. Soc.* **1995**, *117*, 486.

(25) (a) Dolg, M.; Wedig, U.; Stoll, H.; Preuss, H. *J. Chem. Phys.* **1987**, *86*, 866. (b) Schwerdtfeger, P.; Dolg, M.; Schwarz, W. H.; Bowmaker, G. A.; Boyd, P. D. W. *J. Chem. Phys.* **1989**, *91*, 1762. (c) Andrae, D.; Haubermann, U.; Dolg, M.; Stoll, H.; Preuss, H. *Theor. Chim. Acta* **1990**, *77*, 123. (d) Bergner, A.; Dolg, M.; Kÿchle, W.; Stoll, H.; Preuss, H. *Mol. Phys.* **1993**, *80*, 1431.

(26) Ehlers, A. W.; Bohme, M.; Dapprich, S.; Gobbi, A.; Hollwarth, A.; Jonas, V.; Kohler, K. F.; Stegmann, R.; Veldkamp, A.; Freking, G. *Chem. Phys. Lett.* **1993**, 208, 111.

(27) Frisch, M. J.; et al. *Gaussian 03*, revision C.02; Gaussian, Inc.: Wallingford, CT, 2004.

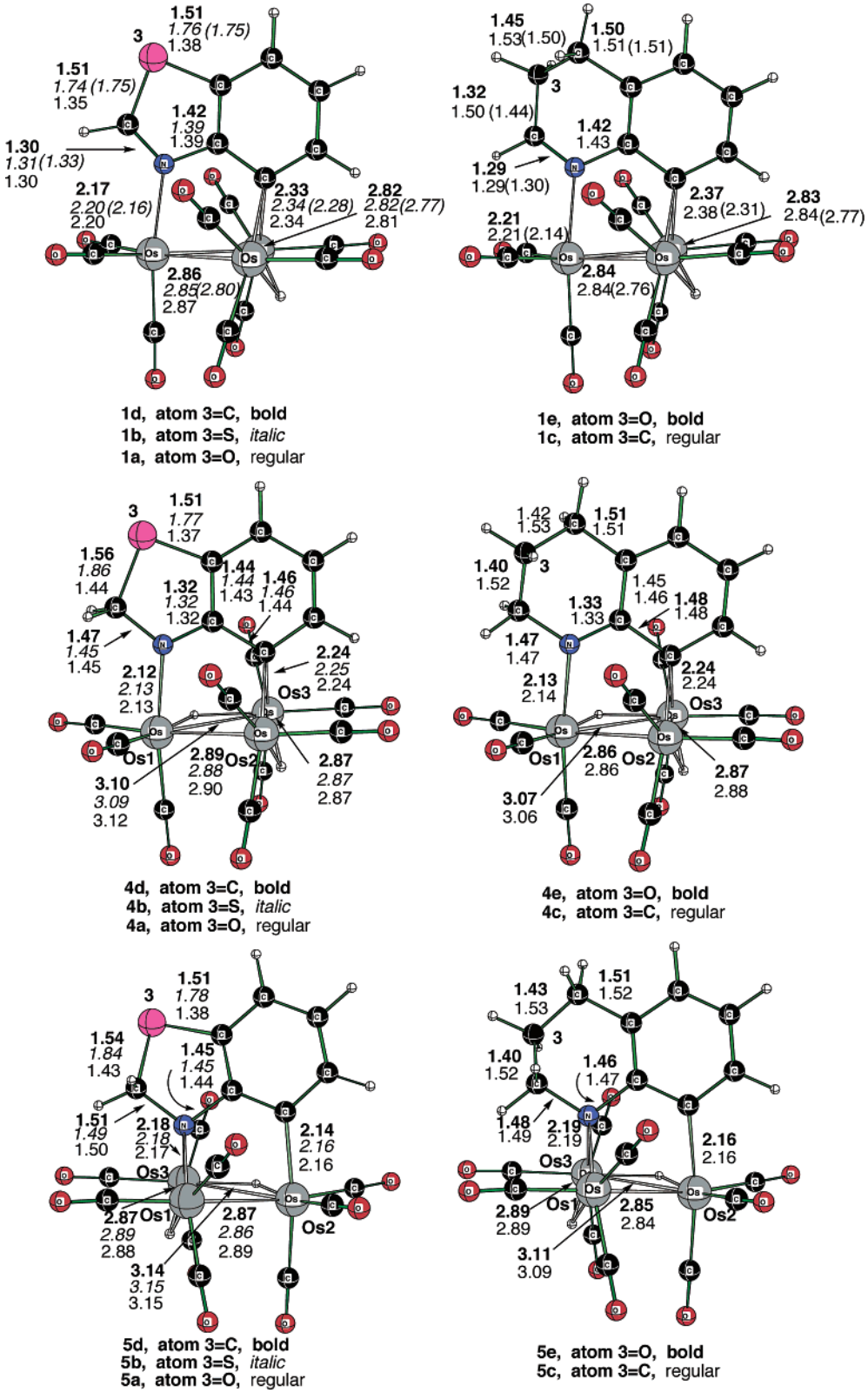

Figure 1. Calculated and experimental (in parentheses) structures (with bond distances in Å) of the 46-electron reactant complexes **1a**−**e** and two products resulting from sequential H^-/H^+ addition of products, alkylideneimino complexes **4a**−**e**, and amidoaryl complexes **5a**−**e**.

In Table 2, one finds that the difference in the energy of reaction between **1a**−**e** + H_2 → **4a**−**e** and → **5a**−**e** or the thermodynamic energy difference between the isomeric products **4** and **5**, for each organic ligand from **a** to **e**, is very small, with differences of about 1 kcal/mol for all ligands from **a** to **d** and 4 kcal/mol for **e**. Obviously, these small differences are beyond the accuracy of the B3LYP method and will not be discussed further. However, it qualitatively shows that both products **4a**−**e** and **5a**−**e** have almost an equal chance to occur from the thermodynamic

Table 1. Net Charge by NPA for the 46-Electron Reactant Complexes **1a**−**e**[a]

complex	Os1	Os	Os3	N	C2	X3	C8	C10
1a	−0.06	−0.11	−0.11	−0.52	+0.68	−0.45 (X = O)	−0.46	+0.14
1b	−0.06	−0.11	−0.11	−0.49	+0.17	+0.48 (X = S)	−0.46	+0.18
1c	−0.05	−0.09	−0.11	−0.48	+0.43	+0.11 (X = C)	−0.45	+0.19
1d	−0.06	−0.11	−0.11	−0.47	+0.42	−0.06 (X = C)	−0.47	+0.20
1e	−0.06	−0.10	−0.11	−0.56	+0.73	−0.50 (X = O)	−0.46	+0.20

[a] The reported charges on C are the sum of the C and H charges at each ring position.

Table 2. Enthalpy and Free Energy (in kcal/mol at 298.15 K and 1 atm) of Formation of μ_3-η^2-Alkylideneimino (**4a**−**e**) and μ_3-η^2-Amidoaryl (**5a**−**e**) Complexes with Respect to the Reactant Complex **1a**−**e**[a]

	4		**5**	
complex	ΔH	ΔG	ΔH	ΔG
a	−8.1	+1.0	−7.7	+2.2
b	−7.3	+1.7	−7.1	+2.8
c	−15.3	−5.6	−14.9	−4.2
d	−15.2	−6.3	−16.1	−6.2
e	−9.0	+0.9	−13.7	−3.0

[a] The energy of $H^- + H^+$ is assumed to be that of the H_2 molecule (see the text for details).

point of view. For benzoxazole (**a**) and benzothiazole (**b**), the reaction with H_2 is about 8−9 kcal/mol less exothermic in comparison to dihydroquinoline (**c**) and 1,3-dehydroindoline (**d**).

So far, the thermodynamic results show no significant difference between the two kinds of products, **4a**−**e** and **5a**−**e**. Therefore, let us provide a detailed analysis on the observed kinetic products of the two separate steps of the reaction, i.e., the H^- attack and the subsequent protonation of **1a**−**e**.

H^- Addition to the 46-Electron Reactants 1a−**e.** As could be expected from the charge distributions on reactants **1a**−**e** discussed above, the energetically most favorable position for H^- addition is the C2 position of **1a**−**e**, which forms the 48-electron alkyldeneimino anions **2a**−**e**, shown in Figure 2. To gain a better understanding of the H^- addition, we also studied the molecular orbital (MO) characteristics of highest occupied MO (HOMO) and lowest unoccupied MO (LUMO) for the **1a**−**e** structures. In Figure 3, we provide HOMO and LUMO for **1c** as representatives for all studied compounds. Other structures indicate similar characteristics. As is evident, the HOMO of **1c** is completely metal-based in character, while the LUMO consists of contributions from both the metals and ligand and is exposed at the C2 position, as was expected based on NPA.

As is seen in Figure 2, the addition of H^- changes the structure of the ligands by breaking the double bond between C2 and N and forming a new double bond between N and C10. As a consequence, the aromaticity of the carbocyclic ring is disrupted, allowing the formation of an electron-precise (saturated) bridging bond at C8 with two Os atoms along one edge of the cluster. In general, upon going from **1a**−**e** to **2a**−**e**, the Os−C8 shortens from 2.35 to 2.26 Å (on average). At the same time, the Os−N bond length reduces from 2.20 to 2.15 Å (on average). Meanwhile, larger geometrical changes occur in the intraligand bond distances as a result of the broken aromatic ring (see Figures 1 and 2).

The NPA (Table 1 for **1a**−**e** and Table 3 for **2a**−**e**) indicates a generally significant increase of the electron density at C8, X3 (S, O, C), C2, and N atoms of the organic ligands in **2a**−**e**, while there is a slight decrease of the negative charge on the metals. This suggests that most of the negative charge is retained in the ligand rather than transferred to the metal core. In the case of benzothiazole (**1b**), there is a higher positive charge accumulated on S (+0.48) than on C2 (+0.17). Although S does not tend to be three-coordinate, we examined the addition of H^- to S and, as expected, it caused the ring to break (the resulting structure is about 363 kcal/mol higher in energy compared to the case where H^- is added to the C2 position). Meanwhile, it is also interesting to note that, for clusters **1a**−**e**, the Os metals are almost neutral. Nevertheless, we examined the possibility of the addition of H^- to the metal core. The optimized anionic structure lost the C8 bridge bonds between the Os2 and Os3 metals, and instead a CO bridge is formed between Os1 and Os2. This structure is about 23 kcal/mol higher in energy compared to the case where H^- is added to the C2 position.

So far, our computational studies indicate that H^- addition at the C2 position leads to the most stable intermediate for the clusters **1a**−**e**, which is in accord with previous experimental and theoretical evidence.[9] The exothermicity of the H^- addition reaction **1a**−**e** + H^- → **2a**−**e** is calculated and reported as the measure of the electron affinity of such electron-deficient clusters. The reaction is more exothermic for **c** and **e** clusters with (6,6) ligands, showing an average of 146 kcal/mol. The exothermicity is decreased to 142 kcal/mol (on average) for **a**, **b**, and **d** clusters with (5,6) ligands.

Furthermore, a comparison between bond lengths of anionic **2a**−**e** and neutral **4a**−**e** clusters indicates one major difference, that is, a shorter Os1−Os3 bond length in the anionic structures (2.88 Å on average) compared with the same one in neutral complexes (3.09 Å on average). This could be explained by the lack of bridging H in the anionic cluster. At the same time, the Os1−N, Os2−C8, and Os3−C8 bond lengths are slightly increased, by about 0.02 Å. This, in general, shows stronger metal−metal and weaker metal−ligand bonding in the anionic structures **2a**−**e** compared to the neutral clusters **4a**−**e**.

Thus, H^- addition to **1a**−**e** leads to anions **2a**−**e**, the structures of which resemble the neutral μ_3-η^2-alkylideneimino tautomers **4a**−**e**. However, 48-electron anions may also have isomers (not directly formed from H^- addition to **1a**−**e**) with structures that resemble the amidoaryl tautomers **5a**−**e**. Let us discuss these isomers of the 48-electron anions in detail. As shown in Figure 2, two possible isomers of the 48-electron anions, i.e., **3a**−**e** and **3′a**−**e**, are obtained by removing a H^+ from the Os1−Os3 and Os2−Os3 edges of the **5a**−**e** clusters, respectively.

The optimized structures of anions **3a**−**e** and **3′a**−**e** are very similar to the structure of the starting neutral μ_3-η^2-

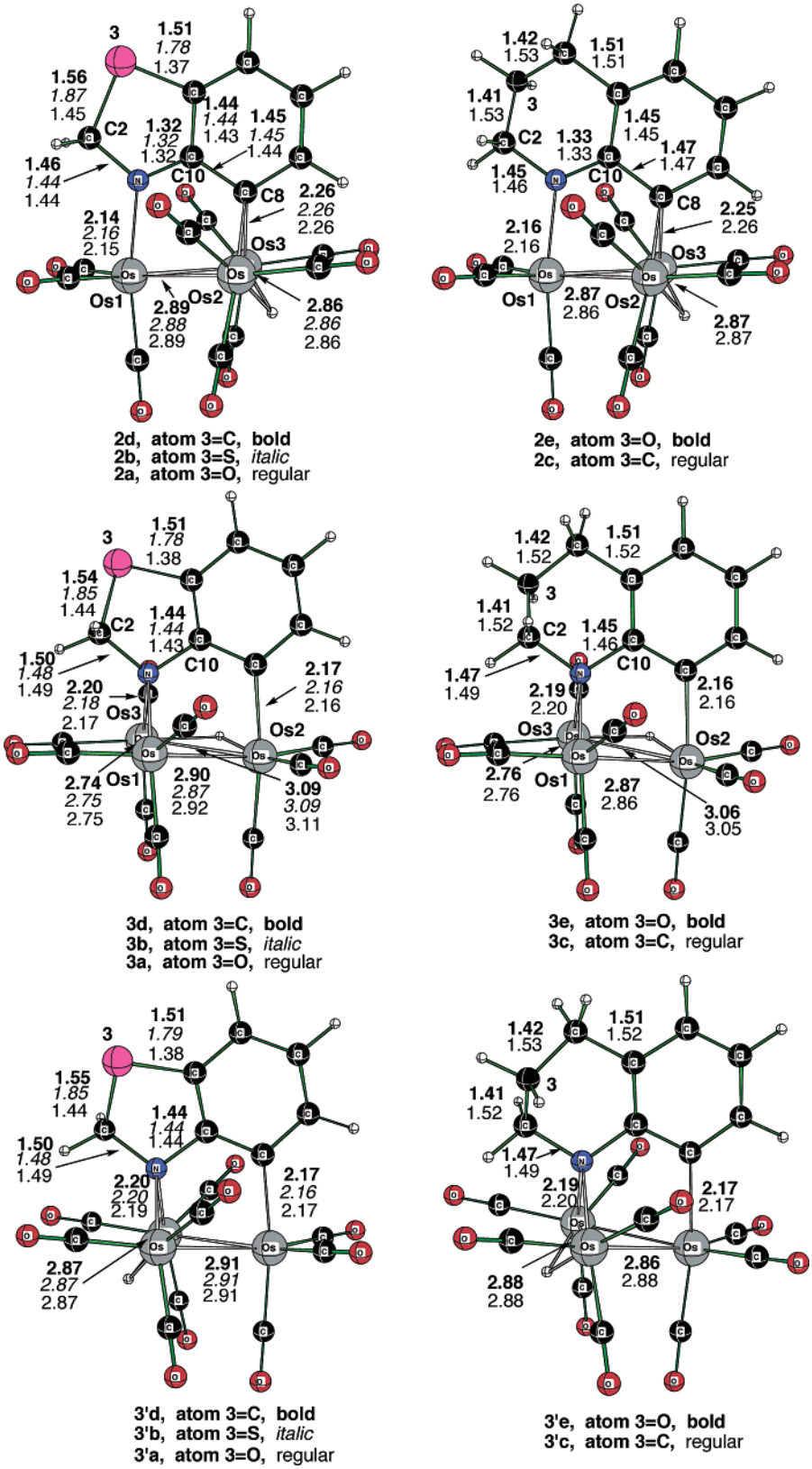

Figure 2. Calculated structures (with bond distances in Å) of the alkylideneimino anions **2a**−**e** and two forms of amidoaryl **3a**−**e** and **3′a**−**e**.

amidoaryl complex. The major difference in the geometries of anionic **3a**−**e** from **5a**−**e** is a significant decrease of the Os1−Os3 bonds, on average from 2.88 to 2.75 Å. This is accompanied by a 0.05-Å decrease in the Os2−Os3 bond and a 0.02-Å increase in the Os1−Os2 bond. Bond-length changes between the metal and ligand and within the heterocycle are not significant. Meanwhile, deprotonation from the Os2−Os3 edge leads to almost symmetrical structures **3′a**−**e** with approximately equal Os1−Os2 and Os2−Os3 bond lengths.

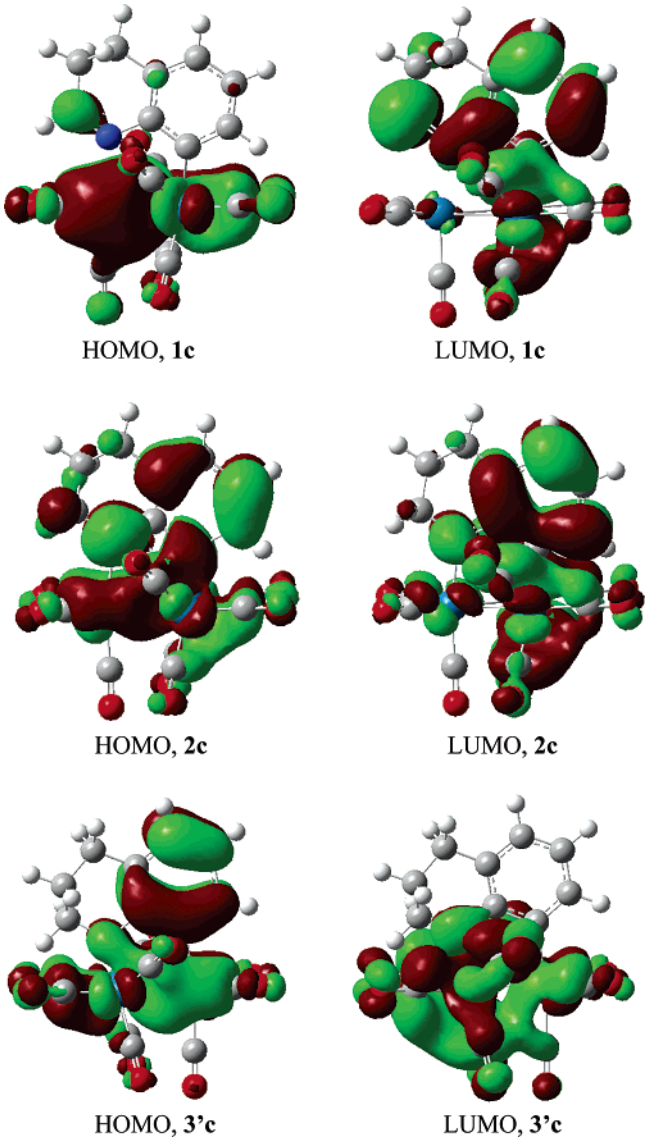

Figure 3. MOs of HOMO and LUMO for 46-electron reactant complex **1c** and for 48-electron alkylideneimino anions **2c** and amidoaryl **3′c**.

Table 3. Net Charge by NPA for the 48-Electron H^- Complexes, Alkylideneimino Anions **2a**−**e**[a]

complex	Os1	Os2	Os3	N	C2	X3	C8	C10
2a	−0.03	−0.08	−0.08	−0.59	+0.51	−0.53 (X = O)	−0.55	+0.23
2b	−0.02	−0.08	−0.08	−0.57	+0.11	+0.23 (X = S)	−0.54	+0.27
2c	−0.02	−0.08	−0.08	−0.57	+0.20	−0.02 (X = C)	−0.54	+0.27
2d	−0.02	−0.08	−0.08	−0.56	+0.21	−0.02 (X = C)	−0.55	+0.27
2e	−0.02	−0.08	−0.08	−0.60	+0.50	−0.58 (X = O)	−0.54	+0.27

[a] The reported charges on C are the sum of the C and H charges at each ring position.

The relative energies of both sets of anions with respect to the previously obtained μ_3-η^2-alkylideneimino anions, **2a**−**e**, are shown in Table 4. It can be seen that the energy differences between the two sets of amidoaryl anions, **3**'s and **3′**'s, are less than 1 kcal/mol. As could be predicted from the energy difference between neutral tautomers (Table 1), the μ_3-η^2-amidoaryl anions are, in general, slightly more stable than μ_3-η^2-alkylideneimino anions.

Transition-State (TS) Structures for the Tautomerization of the Anions. Now that both sets of optimized structures of alkylideneimino anions **2a**−**e** and amidoaryl **3a**−**e** and **3′a**−**e** have been obtained, we investigated the energetic barrier associated with tautomerization of these anionic 48-electron clusters. Previously, the TS for tautomerization of neutral μ_3-η^2-alkylideneimino to μ_3-η^2-amidoaryl has been located for benzoxazole and dehydroindoline ligands,[9] and the energy barriers were calculated to be 30.7 (30.6) and 31.2 (31.5) kcal/mol, respectively. Our calculations show that the barrier for tautomerization of neutral μ_3-η^2-alkylideneimino to μ_3-η^2-amidoaryl for the tetrahydroquinoline ligand is 34.7 (34.6) kcal/mol. For the sake of comparison, we determined TSs **2a-to-3a**, **2b-to-3b**, and **2c-to-3c** for the interconversion of μ_3-η^2-alkylideneimino to μ_3-η^2-amidoaryl anions. The optimized TS structures are provided in Figure 4, where arrows show reaction coordinates. In the case of benzoxazole anions (**a**), the C8−Os3 bond length is increased from 2.26 Å in the anionic alkylideneimino isomer (**2a**) to 2.93 Å in the TS, while the N−Os3 distance is decreased from 3.39 Å (in **2a**) to 2.84 Å (in **3a**), and the N−Os1 and C8−Os2 bond lengths are decreased from 2.15 and 2.26 Å to 2.13 and 2.19 Å, respectively. Similar relative changes were also observed for the tetrahydroquinoline and dehydroindoline cases. NPA results for the key atoms involved in the TS structures are provided in Table S1 of the Supporting Information. Upon going from **2a**, **2c**, and **2d** to the respective TS structures **TS (2a-to-3a)**, **TS (2c-to-3c)**, and **TS (2d-to-3d)**, there is a notable increase in the negative charge at N (average $\Delta Q = -0.13$) as well as a significant decrease in the negative charge at C8 (average $\Delta Q = 0.16$). Although other changes are insignificant, in general the electron densities of the TS structures resemble those of the amidoaryl anions **3a**, **3c**, and **3d** (see Table S2 of the Supporting Information) rather than the starting alkylideneimino anions **2a**, **2c**, and **2d** (Table 3).

Table 4. Enthalpy and Free Energy (in kcal/mol at 298.15 K and 1 atm) of Formation of Amidoaryl Anions **3a**−**e** and **3′a**−**e** with Respect to Alkylideneimino Anions **2a**−**e**

	3		**3′**	
complex	ΔH	ΔG	ΔH	ΔG
a	−2.6	−1.7	−2.1	−1.2
b	−1.3	−0.3	−1.4	−0.4
c	−1.2	−0.1	−3.2	−1.9
d	−4.0	−2.5	−3.9	−2.4
e	−4.8	−3.8	−5.9	−4.8

The energy barriers (see Figure 4) for tautomerization of anionic intermediates of benzoxazole, tetrahydroquinoline, and dehydroindoline calculated from the μ_3-η^2-alkylideneimino isomer are significantly lower than those of their neutral counterparts, 26.7 (27.1), 30.7 (30.9), and 26.9 (27.7) kcal/mol, respectively.[9] This could be a result of the decreased metal−metal bond lengths associated with the anions, which would require smaller adjustments in the TS structure.

Given the calculated Gibbs free energy barriers for tautomerization, an estimate of the rate constant at 25 °C

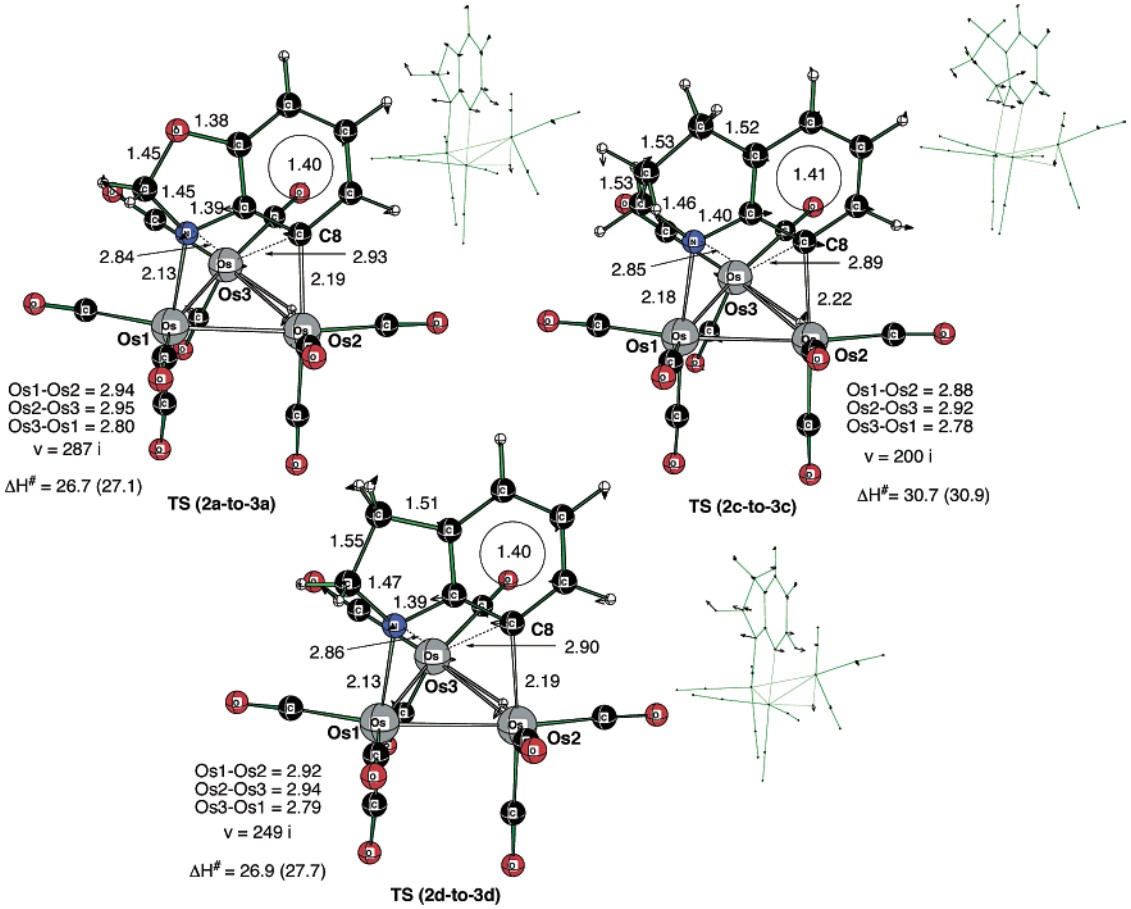

Figure 4. Enthalpy (free energy in parentheses, in kcal/mol) of activation and the calculated structures (with bond distances in Å) of the TSs for interconversion of the alkylideneimino anions **2a**, **2c**, and **2d** to the amidoaryl anions **3a**, **3c**, and **3d**. The arrows show the reaction coordinate, the imaginary vibrational frequency of which is given in cm^{-1}.

Table 5. Relative Enthalpy (Free Energy in Parentheses) of the Neutral Species Resulting from Protonation of Alkylideneimino Anions **2c**, **2a**, and **2b** and Amidoaryl Anions **3′c**, **3′a**, and **3′b** at Different Sites[a]

complex	Os1−Os2	Os1−Os3	N front	N back	Os1	Mid-Os triangle	C8
alkylideneimino **2c**	0.0 (0.0)	0.5 (0.4)	6.2 (6.1)	3.4 (3.2)	11.3 (11.6)	16.5 (17.4)	22.9 (22.5)
amidoaryl **3′c**	0.4 (1.4)	1.7 (2.4)	7.9 (7.1)		11.7 (13.0)	15.4 (17.4)	7.5 (7.6)
alkylideneimino **2a**	0.0 (0.0)	0.0 (0.0)	8.7 (8.9)	8.7 (8.8)	11.3 (11.8)	16.8 (15.5)	25.2 (24.8)
amidoaryl **3′a**	0.4 (1.1)		8.4 (9.2)		13.0 (14.0)		
alkylideneimino **2b**	0.0 (0.0)		7.6 (7.7)				
amidoaryl **3′b**	0.4 (1.1)		10.6 (10.9)				

[a] **c** = dihydroquinoline, **a** = benzoxazole, **b** = benzothiazole.

can be calculated using the Eyring equation.[28] These values of ca. 10^{-8}−10^{-10} are still too small to account for extraordinary interconversion of the anionic tautomers at 25 °C prior to protonation. In light of the above results, one may expect that the protonation site of 48-electron anionic clusters may play a key role in controlling the nature of the kinetic product.

Protonation of the 48-Electron Anionic Clusters. According to our NPA analysis of the anions **2a**−**e**, **3a**−**e**, and **3′a**−**e** (see Tables 3 and S2 and S3 of the Supporting Information), the highest accumulation of electron density is on the N and C8 positions for all anions. Therefore, it is reasonable to expect that the protonation should take place at either of these two sites. The MOs of HUMO and LUMO for **2e** and **3′e** structures are shown in Figure 3, where HOMOs provide a good insight for possible protonation sites: mostly on metal cores, the N, and the C8. Considering the above data as well as experimental evidences and to determine the most probable protonation site, we performed several sets of calculations for the addition of H^+ to different possible sites in the anions.

For the dihydroquinoline ligand, anionic cluster **3′c** is found to be more stable than **3c**. Therefore, below we mainly concentrate on the protonation of alkylideneimino anion **2c** and amidoaryl anion **3′c** (see Table 5). Optimized structures showing the key geometrical parameters are given in Figures 5 and 6, respectively.

As seen in Figure 5 for alkylideneimino anion **2c**, the addition of H^+ to the center of a two-Os bond vector on the unbridged edges leads to the formation of neutral alkylide-

(28) Stiller, W. *Arrhenius Equation and Nonequilibrium Kinetics*; BSB B. G. Teubner: Leipzig, Germany, 1989; p 16.

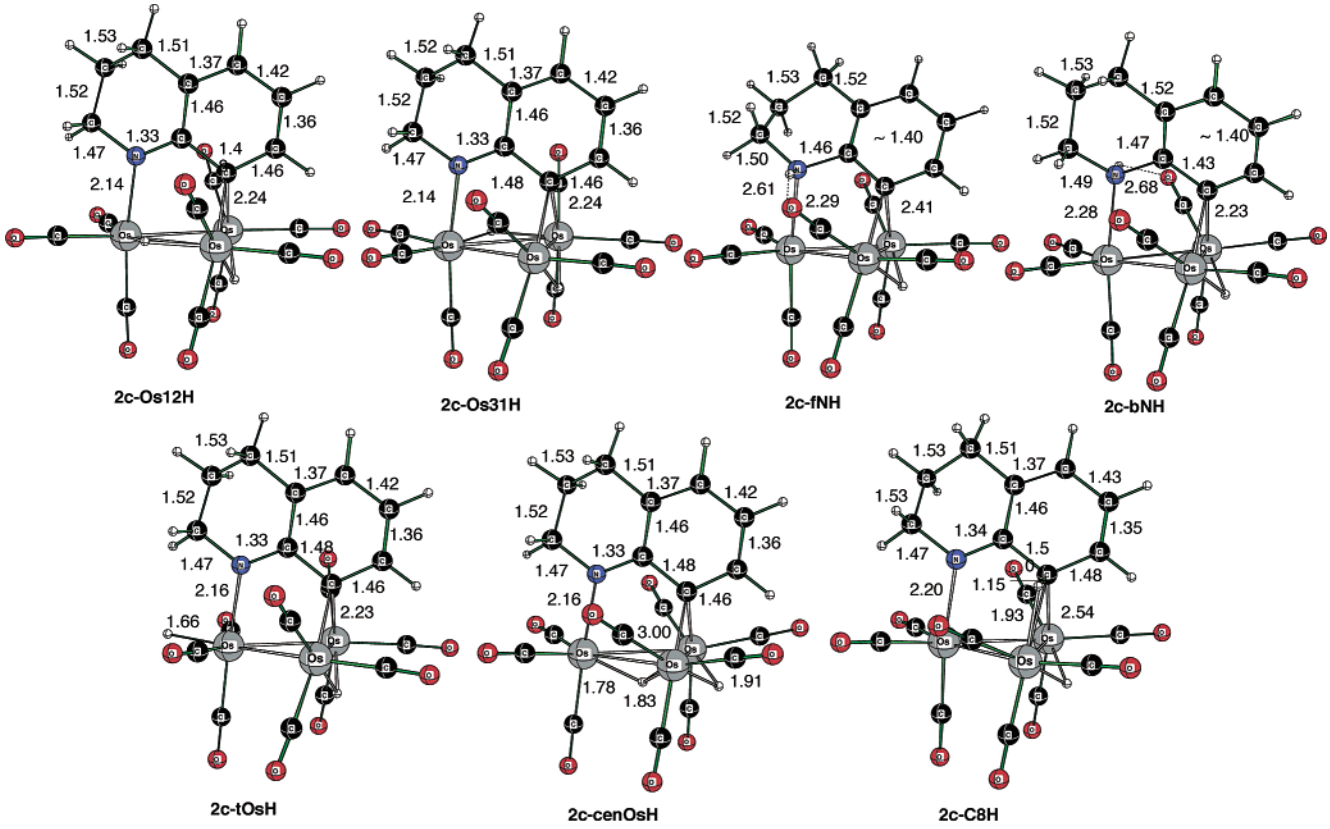

Figure 5. Calculated structures (with bond distances in Å) of the neutral complexes resulting from protonation of the alkylideneimino anion **2c**.

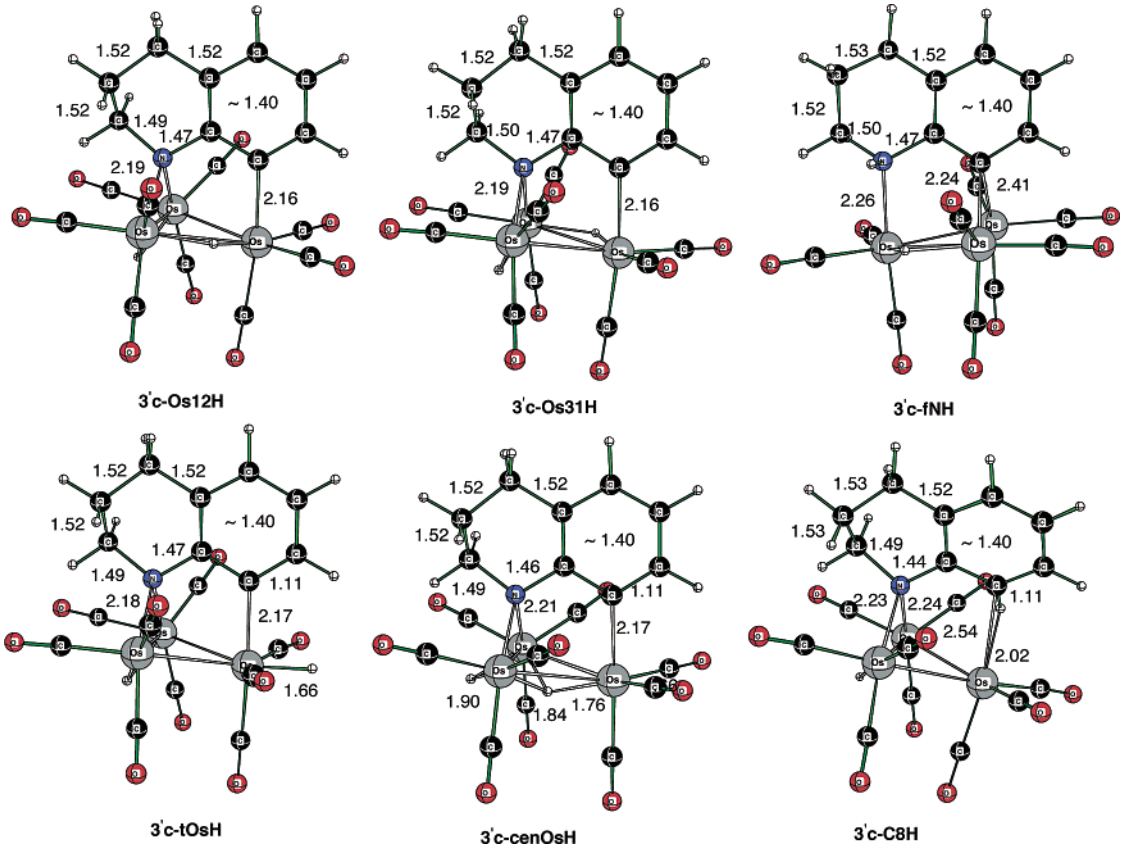

Figure 6. Calculated structures (with bond distances in Å) of the neutral complexes resulting from protonation of amidoaryl anion **3′c**.

neimino clusters **2c-Os12H** or **2c-Os31H** (similar to the product **5c**), where the former is only 0.5 kcal/mol more stable than the latter. This is due to the puckered (6,6) heterocycle structure, which provides a nonsymmetrical

structure. According to NPA (Table S3 of the Supporting Information), the N center has the highest electron density of −0.57e and seems to be the most probable site for protonation. Therefore, we performed the addition of H^+ from both the front and back sides of the N atom. The addition of H^+ to N from the back side leads to a more stable product (∼3 kcal/mol; **2c-bNH**) compared to the front-side addition (**2c-fNH**). Analysis of the geometric parameters shows that in **2c-bNH** the heterocycle is twisted more to resemble a chair conformation.

H^+ addition to Os1 to give a terminal H^-, the center of the Os triangle, and C8 leads to unstable intermediates **2c-tOsH**, **2c-cenOsH**, and **2c-C8H** with energies as high as 11.34, 16.52, and 22.95 kcal/mol relative to the **2c-Os12H** cluster. Because the energy difference between the **2c-Os12H** and **2c-bNH** isomers is only 3.39 kcal/mol, one may conclude that protonation of alkylideneimino anion **2c** may take place both at the metal core, **2c-Os12H**, and at the N atom, **2c-bNH**, during the reaction, eventually leading to a alkylideneimino product.

Next, let us discuss the H^+ addition to amidoaryl anion **3′c** (Figure 6) , where protonation at different Os−Os edges leads to neutral amidoaryl structures **3′c-Os12H** or **3′c-Os31H** with almost the same energies of 0.40 and 1.70 kcal/mol with respect to the reference neutral alkylideneimino **2c-Os12H**. So far, it can be concluded that protonation at the metal core of any anion (**2c** or **3′c**) does not change the bonding mode of the heterocyclic ligand. In contrast, when protonation of amidoaryl anion **3′c** occurs at the N atom, the electronic structure of the ligand is changed and the resulting structure resembles a alkylideneimino cluster. Therefore, one can conclude that if the protonation takes place at N for any anion (**2c** or **3′c**), the resulting neutral intermediate always bears an alkylideneimino bonding mode, regardless of the nature of the initial bonding mode of the ligands in the anions. The addition of H^+ to Os1 to give a terminal H^-, the center of Os triangle, and the C8 of the **3′c** cluster leads to less stable intermediates **3′c-tOsH**, **3′c-C8H**, and **3′c-cenOsH** with energies of 11.68, 15.38, and 7.53 kcal/mol, respectively, with respect to the reference cluster **2c-Os12H**.

We performed the same kind of calculation for benzoxazole anion **2a**. The addition of H^+ to the Os−Os edge leads to **2a-Os12H**, an alkylideneimino cluster. Contrary to the dihydroquinoline case, the addition of H^+ to bridge the Os1−Os2 edge or to bridge the Os2−Os3 edge does not affect the geometry and energy of the obtained intermediate. This is due to the planar structure of the (5,6) ring heterocyclic ligand, providing an almost symmetrical environment on both sides. For the same reason, both intermediates resulting from protonation of the N atom from the front side (**2a-fNH**) and back side (**2a-bNH**) have almost the same energies of about 8.73 kcal/mol with respect to **2a-Os12H**. As shown in Table 5, when H^+ attacks other positions, higher energy intermediates result, which are not likely to be accessible experimentally.

We also examined the addition of H^+ to the metal core and the N (back side) of amidoaryl for benzoxazole **3′a**. Similar to the alkylideneimino anion **2a** case, H^+ addition to N provides an intermediate with about 8.39 kcal/mol energy higher than that from addition to the metal core.

In general, we can conclude that the most probable protonation site for all studied anions is at the metal edges, while protonation at the N atom could also be accessible at room temperature. This is consistent with experimental observations for the benzothiazole cluster, indicating that protonation occurs at the N atom, followed by H^+ transfer to the metal core. It is likely that this proceeds through a TS structure (not determined) involving considerable N to Os bond formation. The process can be rationalized by participation of the second heteroatom lone pair in electron donation to the metal core. This proposed mechanism is supported by our recent computational results on the TS for hydrogen transfer N−H to Os, in which considerable N−Os bonding is maintained.[21]

In the case of tetrahydroquinoline anion **2c**, it seems that there is no driving force for H^+ transfer from N to the metal core. Therefore, H^+ dissociation and coordination at the metal core results in the formation of the alkylimino as the kinetic product.

Our discussions on the protonation site were only based on the relative stabilities of the intermediates. Obviously, the energetics of TS structures for H^+ transfer from N to Os is required for more quantitative discussion and will be the subject of a future study.

4. Conclusions

From the results and discussion presented above, we can draw the following conclusions.

1. The enthalpies of formation of **4a**−**e** or **5a**−**e** from **1a**−**e** complexes by sequential H^- and H^+ addition are qualitatively similar for all of the studied ligands (L = benzoxazole, **1a**; benzothiazole, **1b**; dihydroquinoline, **1c**; 1,2-dehydroindoline, **1d**; 4*H*-3,1-benzoxazine, **1e**). Those of **4a**, **4b**, **5a**, and **5b** with a (5,6) ring and an additional heteroatom, such as benzoxazole and benzothiazole, are about 8−9 kcal/mol smaller than those for dihydroquinoline, 1,2-dehydroindoline, and 4*H*-3,1-benzoxazine ligands. These results indicate that two kinds of products, **4a**−**e** and **5a**−**e**, are accessible from the thermodynamic point of view.

2. H^- addition at the C2 position for all heterocycles leads to the most stable isomer, **2a**−**e**, indicating that all of them have the same μ_3-η^2-alkylideneimino structure. Thus, this nucleophilic attack does not determine the structure of the neutral kinetic product formed after protonation.

3. Deprotonation of μ_3-η^2-amidoaryl complex **5a**−**e**, from different sites of bridging Os1−Os3 or Os2−O3 edge, leads to a structure almost similar to that of the initial μ_3-η^2-amidoaryl complex. This result proves that deprotonation does not play a role in triggering the interconversion of the two tautomeric anions.

4. Alkylideneimino to amidoaryl tautomerization in anionic structures bearing benzoxazole, tetrahydroquinoline, and dehydroindoline ligands occurs via the TS that is very similar to that for neutral cases previously reported. The calculated activation barriers, 26.7−26.9 kcal/mol, are significantly

smaller than those for neutral clusters. However, the barriers are still too high to account for anionic tautomerization at room temperature.

5. Protonation of dihydroquinolinealkylideneimino and dihydroquinolineamidoaryl anions might take place either at the N atom or at the metal core. The situation is different for benzothiazole and benzoxazole clusters, where H^+ transfer from N to the metal core involves considerable N to Os bond formation.

Taken together with the results of the two previous papers in this series, the results reported here show that the DFT method can provide useful information on the reaction energetics of ligand−cluster reactions and insight into their subsequent rearrangements and reactivities with small molecules.[9,21] Still lacking are generalizations regarding the nature of the TSs involved in ligand-to-metal and metal-to-ligand hydrogen transfers as well as methods for handling multistep transformations of a concerted nature.[13−15] These investigations are currently underway in our laboratories.

Acknowledgment. Support for this research by the Department of Energy (to E.R. under Grant DE-FG02-01E.R.45869) and the National Science Foundation (to K.M. and D.G.M. under Grant CHE-0209660) is gratefully acknowledged. E.R. thanks the Cherry Emerson Center for Scientific Computation for a Visiting Fellowship Award. A DURIP grant (FA9550-04-1-0321) from AFOSR is also acknowledged for support of the computer facilities. The use of computational resources at the Cherry Emerson Center for Scientific Computation is also acknowledged.

Supporting Information Available: Calculated and experimental (in parentheses) structures of the 46-electron reactant complexes **1b** and **1c** optimized at B3LYP/SDD+6-31G(d) (Figure F1), NPA for TS structures **2*x*-to-3*x***, where ***x*** = **a**, **c**, **d**, for amidoaryl anions **3a**−**e** and **3′a**−**e**, and for the 46-electron reactant complexes **1c**, for alkylideneimino anions **2c**, for amidoaryl anions **3c** and **3c′**, and TS structures **2c-to-3c** at B3LYP/ SDD+6-31G(d) (Tables S1−S4), enthalpy and free energy (at 298.15 K and 1 atm) of formation of μ_3-η^2-alkylideneimino **4c** and μ_3-η^2-amidoaryl **5c** complexes with respect to the reactant complex **1c** and of formation of amidoaryl anions **3c** and **3′c** with respect to alkylideneimino anion **2c**, calculated at B3LYP/ SDD+6-31G(d) (Table S5), and Cartesian coordinates of all structures reported in this paper (Table S6). This material is available free of charge via the Internet at http://pubs.acs.org.

IC052012X